

Lactic Acid- and Carbonate-Based Crosslinked Polymeric Micelles for Drug Delivery

Michael Danquah,¹ Tomoko Fujiwara,² Ram I. Mahato¹

¹Department of Pharmaceutical Sciences, University of Tennessee Health Science Center, Memphis, Tennessee, 38103

²Department of Chemistry, The University of Memphis, Memphis, Tennessee 38152

Correspondence to: R. I. Mahato 19 South Manassas, CRB RM 224, Memphis, Tennessee 38103-3308 (E-mail: rmahato@uthsc.edu)

Received 4 June 2012; accepted 12 September 2012; published online 19 October 2012

DOI: 10.1002/pola.26392

ABSTRACT: Our objective was to synthesize and evaluate lactic acid- and carbonate-based biodegradable core- and core-corona crosslinkable copolymers for anticancer drug delivery. Methoxy poly(ethylene glycol)-*b*-poly(carbonate-*co*-lactide-*co*-5-methyl-5-allyloxycarbonyl-1,3-dioxane-2-one) [mPEG-*b*-P(CB-*co*-LA-*co*-MAC)] and methoxy poly(ethylene glycol)-*b*-poly(acryloyl carbonate)-*b*-poly(carbonate-*co*-lactide) [mPEG-*b*-PMAC-*b*-P(CB-*co*-LA)] copolymers were synthesized by ring-opening polymerization of LA, CB, and MAC using mPEG as a macroinitiator and 1,8-diazabicycloundec-7-ene as a catalyst. These amphiphilic copolymers which exhibited low polydispersity and critical micelle concentration values (0.8–1 mg/L) were used to prepare micelles with or without drug and stabilized by crosslinking via radical polymerization of double bonds introduced in the core and interface to improve stability. mPEG₁₁₄-*b*-P(CB₉-*co*-LA₃₅-*co*-MAC_{2.5}) had a higher drug encapsulation efficiency (78.72% ± 0.15%) compared to mPEG₁₁₄-*b*-

PMAC_{2.5}-*b*-P(CB₉-*co*-LA₃₉) (20.29% ± 0.11%).¹H NMR and IR spectroscopy confirmed successful crosslinking (~70%) while light scattering and transmission electron microscopy were used to determine micelle size and morphology. Crosslinked micelles demonstrated enhanced stability against extensive dilution with aqueous solvents and in the presence of physiological simulating serum concentration. Furthermore, bicalutamide-loaded crosslinked micelles were more potent compared to non-crosslinked micelles in inhibiting LNCaP cell proliferation irrespective of polymer type. Finally, these results suggest crosslinked micelles to be promising drug delivery vehicles for chemotherapy. © 2012 Wiley Periodicals, Inc. *J Polym Sci Part A: Polym Chem* 51: 347–362, 2013

KEYWORDS: biomaterials; core-crosslinked micelles; drug delivery systems; interface-crosslinked micelles; micelles; polycarbonate; poly lactic acid

INTRODUCTION Polymeric micelles are presently under intense investigation as nanovehicles for delivery of low-molecular weight chemotherapeutic drugs. Key advantages of polymeric micelles include efficient solubilization of hydrophobic agents in their core^{1–3} and the ability to be made site-specific. Furthermore, they are nanosized supramolecules which self-assemble into core-corona structures from amphiphilic block copolymers above the critical micelle concentration (CMC).³ These intrinsic physicochemical properties of micelles often leads to prolonged blood circulation kinetics⁴ and preferential tumor accumulation via the enhanced permeation and retention effect.^{5–7} Nonetheless, poor *in vivo* stability resulting in premature dissociation and subsequent untimely drug release has limited their clinical application.^{8–11} Polymeric micelles become unstable either due to destabilization by plasma proteins (kinetic instability) or dilutions below their CMC (thermodynamic instability) upon systemic administration.

To facilitate clinical translation of polymeric micelle-based therapeutics, recent research effort has focused on increasing

micelle thermodynamic and kinetic stability using physical or chemical strategies. As micelles with low CMC values have better thermodynamic stability, typical physical approaches involve strategically altering properties of amphiphilic copolymers, which can affect the CMC (e.g., chain length and chemical composition).^{12,13} For example, tailoring the hydrophobic core to contain aromatic moieties has been shown to improve micelle stability through π - π interactions as demonstrated by decreased CMC values.¹² In practice, physically stabilized micelles are limited by their inability to prevent micelle destabilization caused by blood components.

In contrast, introduction of chemical covalent crosslinks into the shell, core, or core-corona interface of micelles is a potential approach to stabilize micelles against both plasma proteins and sub-CMCs.^{13–16} Over the past decade, shell-crosslinked micelles have been extensively studied.¹⁷ It has been shown that shell-crosslinked micelles remain stable upon infinite dilution compared to precursor micelles. High core mobility, greater versatility in core composition and

Additional Supporting Information may be found in the online version of this article.

© 2012 Wiley Periodicals, Inc.

properties, and the membrane-like characteristics of the crosslinked shell layer, which can improve encapsulation are advantages associated with shell-crosslinked micelles. However, one longstanding issue with shell-crosslinked micelles is their low crosslinking efficiency due to their need to be prepared at high dilution to prevent intermicellar crosslinking. Furthermore, shell crosslinking tends to suppress the mobility of the hydrophilic corona chains (e.g., poly(ethylene glycol) [PEG]).

Core-crosslinked micelles exhibit better crosslinking efficiencies as they do not need to be prepared at high dilution to prevent intermicellar crosslinking. Several groups have introduced crosslinkable groups into the hydrophobic portion of the block copolymer which may be polymerized after micellation to lock the micelle structure. For instance, Kataoka's group reported core-crosslinked micelles prepared using poly(ethylene glycol)-*b*-polylactide (PEG-*b*-PLA) possessing methacryloyl groups at the end of the PLA chain.^{18,19} These methacryloyl groups could be photopolymerized using ultraviolet (UV) light or polymerized thermally via the addition of a radical initiator. In another paper, Hu et al.²⁰ covalently stabilized micelle architecture using a hydrophobic polymer block containing crosslinkable double bonds. Recently, Garg et al.²¹ used click chemistry to introduce hydrolyzable crosslinks in the core of poly(ethylene oxide)-*block*-poly(ϵ -caprolactone) (PEO-*b*-PCL) micelles. These crosslinked micelles also demonstrated enhanced stability under diluted conditions without any detrimental effect on the drug encapsulation and *in vitro* drug release profiles.

Armes and coworkers²² have elegantly stabilized micelles by crosslinking the core-corona interface using triblock copolymers in which the reactive groups capable of undergoing crosslinking are located in the central block. Interfacial crosslinking is potentially more beneficial than shell- or core-crosslinked micelles as it combines the advantages of both methods and may be prepared at high concentrations without intermicellar crosslinking and aggregation. In another study, Xu and coworkers showed reduction-sensitive reversibly interfacially crosslinked micelles to be stable against extensive dilution and physiological salt conditions and retained most drugs even at concentrations below the CMC.²³ Yang et al.²⁴ recently reported preparing interface-crosslinked micelles using PEG-*b*-poly(acryloyl carbonate)-*b*-polycaprolactone (PEG-*b*-PAC-*b*-PCL) triblock copolymer. Once micelles were prepared, the double bonds in the acryloyl carbonate were photo-crosslinked using UV light and a photoinitiator.

Our group has developed a series of thermodynamically stable (low CMCs) lactic acid- and carbonate-based copolymers for micellar drug delivery.^{12,25} To further enhance micelle stability and controlled drug release to make our delivery systems clinically relevant, we herein report on the synthesis, characterization, and *in vitro* evaluation of methoxy poly(ethylene glycol)-*b*-poly(carbonate-*co*-lactide-*co*-5-methyl-5-allyloxycarbonyl-1,3-dioxan-2-one) [mPEG-*b*-P(CB-*co*-LA-*co*-MAC)] and methoxy poly(ethylene glycol)-*b*-poly(5-methyl-5-

allyloxycarbonyl-1,3-dioxan-2-one)-*b*-poly(carbonate-*co*-lactide) [mPEG-*b*-PMAC-*b*-P(CB-*co*-LA)] biodegradable copolymers for core- and core-corona interface-crosslinked micelles. Effect of polymer composition and crosslinking moiety location on key micelle properties was also investigated. Self-aggregation behavior, morphology, and stability of non-crosslinked (NCM) and crosslinked micelles (CM) were determined by dynamic light scattering (DLS), transmission electron microscopy (TEM), proton nuclear magnetic resonance (¹H NMR) spectroscopy, and fluorescence spectroscopy. Furthermore, influence of crosslink location on micelle stability against physiological simulating dilution and serum conditions as well as drug release was investigated.

EXPERIMENTAL

Materials

2,2-bis(Hydroxymethyl) propionic acid, tin(II) 2-ethylhexanoate (Sn(Oct)₂), dimethylaminopyridine, allyl bromide, and benzyl bromide were purchased from Sigma Aldrich (St. Louis, MO) and used as received. mPEG ($M_n = 5000$, polydispersity index [PDI] = 1.03) was obtained from Sigma Aldrich (St. Louis, MO) dried by lyophilization from benzene solution unless it was freshly opened reagent. L-Lactide (LA) was purchased from PURAC Biochem bv (Gorinchem, The Netherlands) and recrystallized from toluene several times. 1-Ethyl-3-(3-dimethylaminopropyl) carbodiimide hydrochloride (EDC) and hydroxybenzotriazole (HOBT) were obtained from AK Scientific (Palo Alto, CA). 1,8-Diazabicyclo[5.4.0]undec-7-ene (DBU) was purchased from Sigma Aldrich, dried over calcium hydride, and distilled. All other reagents were obtained from Sigma Aldrich and used without further purification.

Synthesis of 5-Methyl-5-allyl-1,3-dioxane-2-one

Method 1

5-Methyl-5-benzyloxycarbonyl-1,3-dioxane-2-one (CB) monomer was first synthesized as described by Danquah et al.¹² Briefly, 2,2-bis(hydroxymethyl)propionic acid (0.168 mol) and potassium hydroxide (0.169 mol) were dissolved in 125 mL of dimethylformamide (DMF) by heating at 100 °C for 1 h. Subsequently, benzyl bromide (0.202 mol) was added dropwise to the reaction mixture and allowed to stir at 100 °C for 15 h. The solvent was then removed under reduced pressure, the residue was dissolved in ethyl acetate (150 mL), hexanes (150 mL), and water (100 mL), and dried over Na₂SO₄. The organic layer solvent was removed under vacuum and recrystallized from toluene to yield pure benzyl 2,2-bis(methylol)propionate. Next, benzyl 2,2-bis(methylol)propionate (0.05 mol) was dissolved in a mixture of CH₂Cl₂ (150 mL) and pyridine (25 mL) and the solution chilled to -78 °C. A solution of triphosgene (25 mmol) in CH₂Cl₂ was added dropwise to the reaction mixture over 1 h and stirred for an additional 2 h at the room temperature. The reaction was then quenched with saturated aqueous NH₄Cl (75 mL), and the organic layer was sequentially washed with 1 M aqueous HCl (3 × 100 mL) and saturated aqueous NaHCO₃ (1 × 100 mL), dried with Na₂SO₄, and evaporated under

vacuum to give CB. The crude product was purified by recrystallization from ethyl acetate to obtain white crystals.

5-Methyl-5-allyl-1,3-dioxane-2-one (MAC) monomer was then synthesized by first subjecting CB to catalytic hydrogenation and reacting the subsequent product with allyl alcohol. In brief, CB (3 g) was dissolved in ethyl acetate (30 mL) containing 600 mg Pd/C. The Parr bottle was purged thrice with H₂, charged to 50 psi, and the reaction was allowed to proceed for 3 h. Subsequently, Pd/C catalyst was separated by centrifugation, the solvent was filtered and evaporated under vacuum to give 5-methyl-2-oxo-1,3-dioxane-5-carboxylic acid (MTC-OH) as a white crystal. Next, MTC-OH (3 mmol), allyl alcohol (2.5 mmol), HOBt (3.6 mmol), and EDC (4.5 mmol) were dissolved in DMF (20 mL) to which triethylamine (TEA) (3.5 mmol) was later added, and the reaction was allowed to proceed for 18 h. Afterward, 20 mL of ethyl acetate was added to the mixture and then washed with water. The organic layer was dried over Na₂SO₄, evaporated under vacuum, and the crude product purified by column chromatography to give MAC as white crystals (30%).

Method 2

MAC was synthesized as described by Hu et al.²⁰ Briefly, a mixture of 2,2-bis(hydroxymethyl)propionic acid (9.0 g, 67.11 mmol), potassium hydroxide (88% assay; 4.30 g, 76.79 mmol), and DMF (50 mL) was heated to 100 °C for 1 h with stirring at which point a homogenous potassium salt solution was formed. Allyl bromide (5.8 mL, 67.11 mmol) was added dropwise to the warm solution, and stirring was continued at 45 °C for 48 h. Upon completion of the reaction, the mixture was cooled, solvent was removed under vacuum, and the residue was dissolved in methylene chloride (200 mL) and water (100 mL). The organic layer was retained, washed with water (100 mL), dried (Na₂SO₄), and evaporated to yield a viscous yellowish liquid (70%).

Allyl 2,2-bis(methylol)propionate (10 g, 58 mmol) and ethyl chloroformate (16.5 mL, 0.173 mol) were dissolved in tetrahydrofuran (THF) (200 mL), and the solution was stirred at 0 °C for 30 min under N₂. Subsequently, TEA (24.2 mL, 0.173 mol) was added dropwise over 30 min, after which the reaction mixture was removed from the ice bath and stirred at room temperature overnight. TEA-HCl precipitate was filtered and the filtrate concentrated under reduced pressure. The ensuing solid was recrystallized from THF/ether to obtain white crystals (70%).

Synthesis of mPEG-b-P(Lactide-co-carbonate-co-MAC)

The following reaction mixture was prepared in a fume hood under ambient atmosphere. mPEG (150 mg, 30 μmol), LA (100 mg, 0.693 mmol), CB (100 mg, 0.4 mmol), and MAC (20 mg, 0.1 mmol) were dissolved in CH₂Cl₂ (6 mL) in a 25-mL reaction vessel. DBU (30 μL, 0.2 mmol) was added, and the reaction was carried out for 3 h after which benzoic acid (40 mg, 0.327 mmol) was added. The resulting solution was concentrated to approximately 50% of the initial volume and added dropwise into excess of cold isopropanol with stirring. The polymer was then dried under vacuum.

Synthesis of mPEG-b-PMAC-b-P(Lactide-co-carbonate)

The following reaction mixture was prepared in a fume hood under ambient atmosphere. mPEG (150 mg, 30 μmol) and MAC (40 mg, 0.2 mmol) were dissolved in CH₂Cl₂ (3 mL) in a 25-mL reaction vessel. DBU (15 μL, 0.1 mmol) was added, and the reaction was carried out for 2 h to yield mPEG-*b*-PMAC. To this solution, a mixture (3 mL) of CB (100 mg, 0.4 mmol) and LA (100 mg, 0.693 mmol) was infused into the reaction vessel at a rate of 1 mL/min. DBU (15 μL) was then added, and the reaction was allowed to proceed for 3 h, after which benzoic acid (40 mg, 0.327 mmol) was added. PEG-*b*-PMAC-*b*-P(CB-*co*-LA) copolymer was purified by concentrating the reaction mixture to approximately 50% of the initial volume, added dropwise into excess of cold isopropanol, and dried under vacuum.

Polymer Characterization

NMR

¹H NMR, ¹³C NMR, 2D-COSY, and ¹H-¹³C HSQC spectra were recorded on a Bruker (400 MHz, *T* = 25 °C) using deuterated chloroform (CDCl₃) and deuterated dimethyl sulfoxide (DMSO-*d*₆) as solvents. For crosslinked micelles, they were first prepared, subjected to crosslinking, lyophilized and redissolved in CDCl₃ prior to ¹H NMR studies. The chemical shifts were calibrated using tetramethylsilane as an internal reference and given in parts per million.

Gel Permeation Chromatography

A Shimadzu 20A gel permeation chromatography (GPC) system equipped with two Jordi Gel DVB500 columns and a differential refractive index detector was used to determine the molecular weight and PDI of the copolymers. THF was used as eluent at a flow rate of 1 mL/min at 35 °C. A series of narrow polystyrene standards (900–100,000 g/mol) were used for calibration, and the data were processed using a LcSolution ver.1.21 GPC option software.

Infrared Spectra

Copolymer composition and degree of crosslinking were confirmed with Fourier transform infrared (FTIR) spectra using a Perkin-Elmer FT-IR spectrometer.

CMC

Fluorescence spectroscopy was used to estimate the CMC of mPEG-*b*-P(LA-*co*-CB-*co*-MAC) and mPEG-*b*-PMAC-*b*-P(CB-*co*-LA) copolymers using pyrene as a hydrophobic fluorescent probe as described previously.²⁶ Fluorescence spectra of pyrene were recorded with a Molecular Devices SpectraMax M2/M2e spectrofluorometer (Sunnyvale, CA) with excitation wavelength 338 nm (*I*₃) and 333 nm (*I*₁) and emission wavelength of 390 nm. The intensity ratio (*I*₃/*I*₁) was plotted against the logarithm of polymer concentration and CMC obtained as the point of intersection of two tangents drawn to the curve at high and low concentrations, respectively.

Preparation of Micelles and Crosslinking

mPEG-*b*-P(LA-*co*-CB-*co*-MAC) and mPEG-*b*-PMAC-*b*-P(CB-*co*-LA) micelles were prepared using the film sonication method as previously described with slight modifications.²⁶ Briefly, 20 mg of the copolymer was dissolved in CH₂Cl₂ (2 mL). The

mixture was sonicated for 5 min to ensure homogeneity, and the solvent was evaporated under a flow of N₂. The resulting film was hydrated (10 mL) and sonicated for 10 min using a Misonix ultrasonic liquid processor (Farmingdale, NY) with an amplitude of 70. The ensuing formulation was then centrifuged at 5000 rpm for 10 min and the supernatant filtered using a 0.22- μ m nylon filter.

Micelles were stabilized by polymerization of the allyl moieties. Briefly, the micelle solution was first deoxygenated by bubbling with argon for 1 h. A solution of 2,2-azo-bis(isobutyronitrile) (AIBN) (1.0 wt % of polymer) in THF was then added and stirred for 2 h followed by heating to 70°C for 24 h.

Drug Loading and Encapsulation Efficiency

Bicalutamide-loaded micelles were prepared as described above. 1 mg drug and 19 mg copolymer were dissolved in CH₂Cl₂ (2 mL) and evaporated under a stream of N₂. The film was then hydrated with 10 mL of phosphate buffered saline (PBS), sonicated, and filtered through a 0.22 μ m filter. Acetonitrile was used to extract the loaded drug, and the amount of bicalutamide was determined using UV spectroscopy at 270 nm. Drug loading content and encapsulation efficiency were then determined using eqs 1 and 2 as follows:

$$\begin{aligned} \text{drug loading density (\%)} \\ = \frac{\text{weight of drug in micelles}}{\text{weight of micelles}} \times 100 \end{aligned} \quad (1)$$

$$\begin{aligned} \text{drug encapsulation efficiency (\%)} \\ = \frac{\text{weight of drug in micelles}}{\text{weight of drug originally fed}} \times 100 \end{aligned} \quad (2)$$

Particle Size Distribution and Morphology

Mean particle size (intensity mean) and size distribution of NCM and CM were determined by DLS using a Zetasizer (Malvern Instruments, Worcestershire, UK) at a 1 mg/mL polymer concentration. Samples were analyzed at room temperature with a 90° detection angle, and the mean micelle size was obtained as a Z-average. Five repeat measurements were performed, and data were reported as the mean diameter \pm SD. Zeta potential was measured in PBS (pH = 7.4). NCM and CM micelles prepared using mPEG-*b*-P(LA-*co*-CB-*co*-MAC) and mPEG-*b*-PMAC-*b*-P(CB-*co*-LA) copolymers were visualized using a JEM-100S (Japan) TEM. Micelles were loaded on a copper grid, followed by blotting of excess liquid prior to negative staining with 1% uranyl acetate. The grid was visualized under the electron microscope at 60 kV and magnifications ranging from 50,000 \times to 100,000 \times .

In Vitro Drug Release from Micelles

The dialysis technique was used to study the release profile of bicalutamide from NCM and CM in PBS (pH 7.4) with 0.1% Tween-80. Bicalutamide-loaded micelles with a final bicalutamide concentration of 0.2 mg/ml were placed into a dialysis membrane with a molecular weight cut-off of 2000 Da and dialyzed against 50 mL PBS (pH 7.4) in a thermo-controlled shaker with a stirring speed of 150 rpm. 1 mL samples were taken at specified times and assayed with a

validated UV spectrophotometer by measuring the absorbance of the solution at 270 nm. Samples were injected back into the original media once after being analyzed. The cumulative amount of drug released into the media at each time point was evaluated as the percentage of total drug release to the initial amount of the drug. All experiments were performed in triplicate, and the data were reported as the mean of the three individual experiments.

Assessment of In Vitro Micelle Stability

The stability of NCM and CM in PBS (pH 7.4) and under physiologically simulating conditions (45 mg/mL bovine serum albumin [BSA]) was assessed by DLS. For stability in serum, micelle solution at a final polymer concentration of 20 μ g/mL was incubated in BSA (45 mg/mL) at 37°C for 24 and 48 h with gentle shaking at 100 rpm. Particle size distribution of 1-mL aliquots was determined by DLS ($n = 3$).

In Vitro Cytotoxicity of Bicalutamide-Loaded Micelles

The ability of bicalutamide-loaded PEG-*b*-PMAC-*b*-P(CB-*co*-LA) and PEG-*b*-P(CB-*co*-LA-*co*-MAC) NCM and CM to inhibit cell proliferation was evaluated using LNCaP human prostate cancer cell line. About 3×10^3 cells were incubated with bicalutamide-loaded micelle formulations (0, 25, and 50 μ M of drug) for 24 and 48 h. At the end of treatment, (3-(4,5-Dimethylthiazol-2-yl)-2,5-diphenyltetrazolium bromide, a yellow tetrazole) (MTT) solution (10% v/v) was added to each well, incubated for 4 h, residual formazan crystals were solubilized with DMSO, and the plate was analyzed using a microplate reader (560 nm). Cell viability was expressed as a percentage of control and data reported as the mean of triplicate experiments.

RESULTS

Synthesis and Characterization of MAC

To facilitate micelle stabilization via crosslinking, we synthesized MAC which is a cyclic monomer containing a double bond functional moiety. Figure 1(A) illustrates the reaction pathway for synthesizing the MAC monomer. Drawing from our experience in synthesizing six-membered cyclic carbonate monomers, we first synthesized MAC using *Method 1* according to the procedure previously reported by Pratt et al.²⁷ with slight modification. This method allowed the synthesis of CB intermediate which is an integral component of our lactic acid- and carbonate-based copolymers. To this end, 2,2-bis(hydroxymethyl)propionic acid was reacted with benzyl bromide to give benzyl 2,2-bis(methylol)propionate, which was then reacted with triphosgene to obtain CB (MW: 250 g/mol). The chemical structure of CB was confirmed using mass and ¹H NMR spectroscopy and our results matched the literature.^{12,25} CB was then dehydrogenated using Pd/C catalyst to give MTC-OH (30% of CB) (MW: 160 g/mol). Next, MTC-OH was coupled to allyl alcohol using EDC HOBt chemistry and purified using column chromatography to obtain MAC.

However, as we had large quantities of CB from previous studies, coupled with significant yield drops in step 1C [Fig. 1(A)] and the time consuming column purification step associated with this method, we explored an alternative synthesis route (*Method 2*). In this method, 2,2-bis(hydroxymethyl)propionic

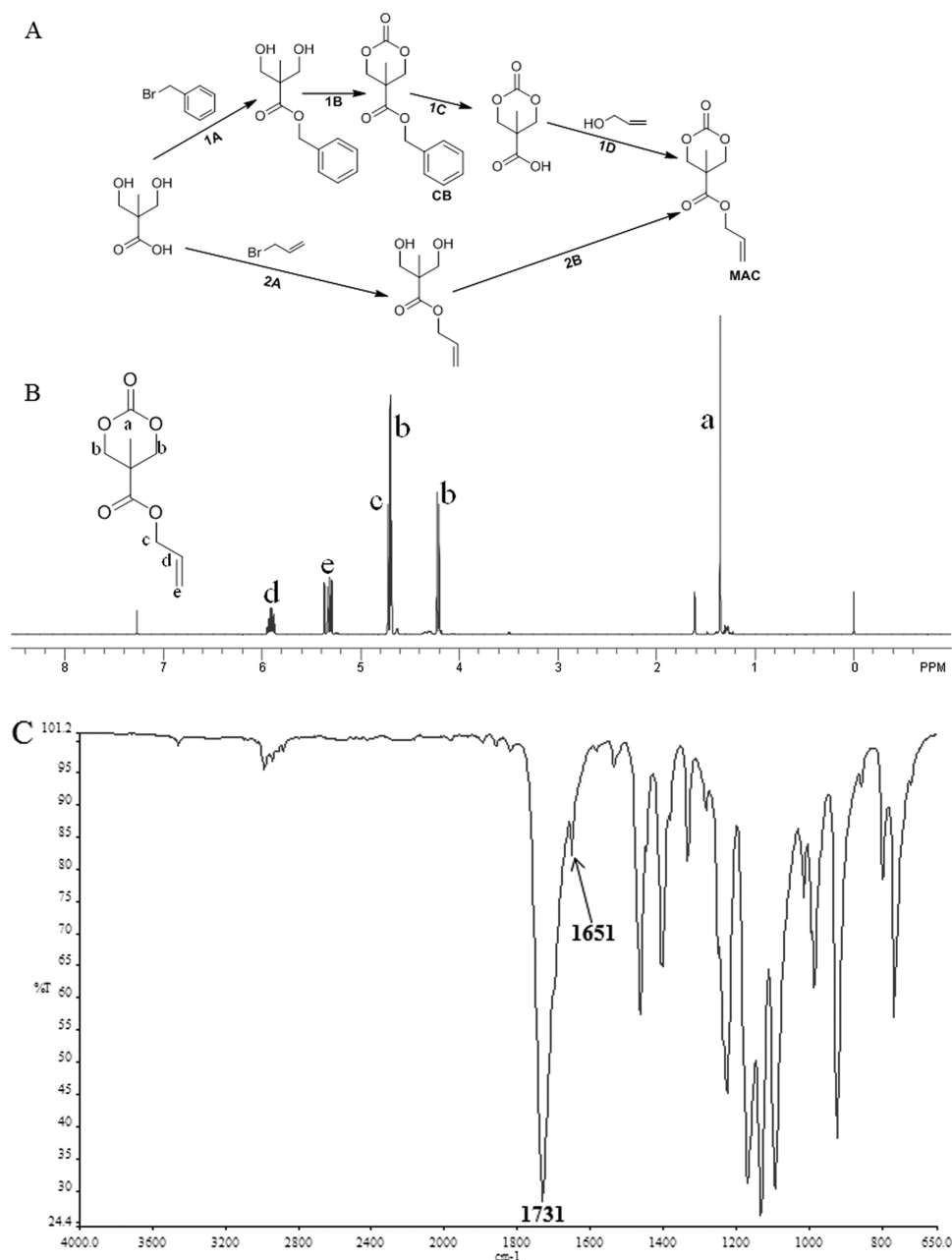


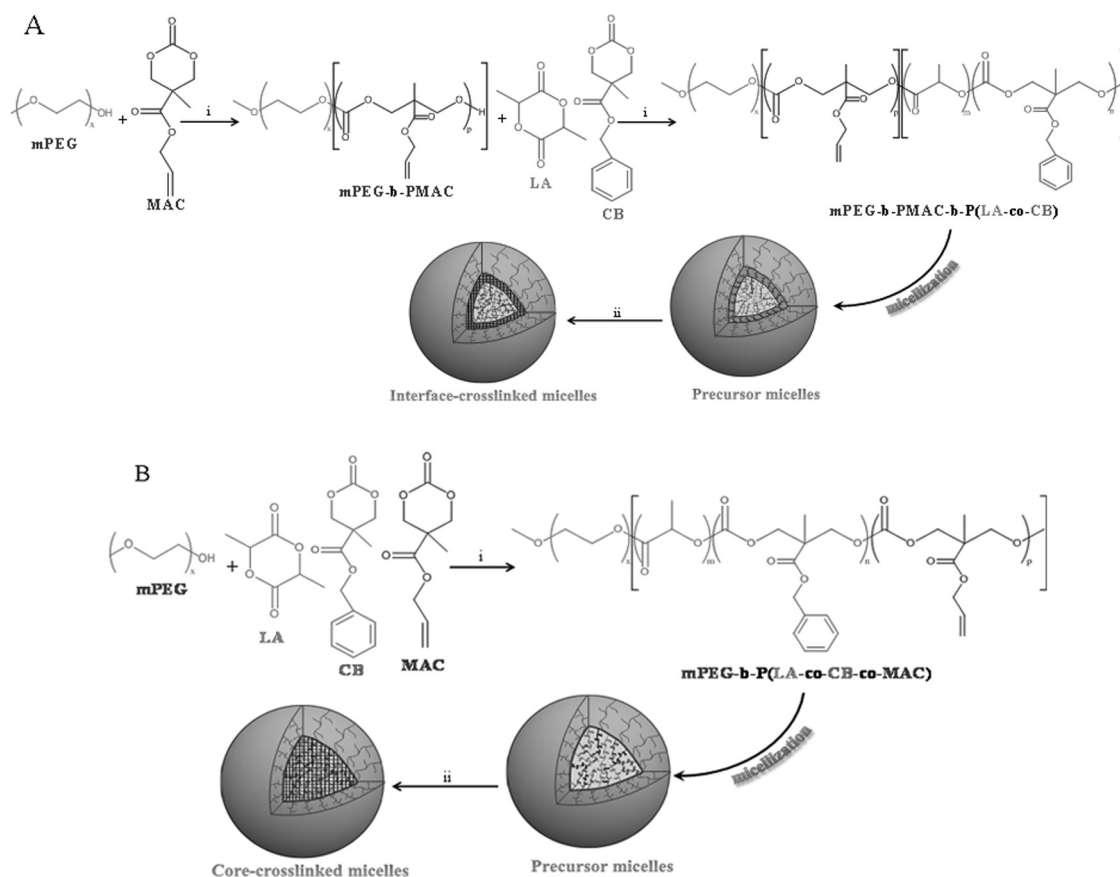
FIGURE 1 (A) Synthesis scheme for MAC. Conditions: (1A) KOH, DMF, 100°C, 15 h. (1B) Triphosgene, pyridine, CH₂Cl₂, –78 to 0°C. (1C) Pd/C (10%), H₂, ethyl acetate, RT, 40 psi, 3 h. (1D) EDC, HOBT, TEA, DMF, RT, 18 h. (2 A) KOH, DMF, preheat to 100°C, 1 h, 45°C, 48 h. (2B) CICO₂Et, THF, TEA, 0°C, 30 min, RT, 12 h. (B) ¹H NMR spectrum of MAC in CDCl₃. (C) FTIR spectrum of MAC.

acid was reacted with allyl bromide to yield allyl 2,2-bis(methylol)propionate (MW: 174 g/mol), which was subsequently reacted with ethyl chloroformate and TEA to give MAC (70%) and purified by recrystallization. Figure 1(B) shows the ¹H NMR spectrum (CDCl₃) of MAC with peak assignments. The signal *d* at 5.8 ppm and *e* at 5.23–5.42 ppm are characteristic of the acryloyl protons in the monomer; while the signal *b* at 4.2 and 4.7 ppm denote methylene protons present in the carbonate ring. Other peak assignments include signals *a* and *c* at 1.38 and 4.72 ppm, assigned to methyl protons in the carbonate ring and methylene protons next to the ester, respectively.

The structure of MAC was further confirmed using FTIR spectrometry [Fig. 1(C)]. Prominent absorbance peaks were observed at 1651 and 1731 cm⁻¹ for C=C and C=O stretches, respectively.

Synthesis and Characterization of mPEG-*b*-PMAC-*b*-P(CB-co-LA) Copolymer

mPEG-*b*-PMAC-*b*-P(CB-co-LA) copolymer was obtained by first reacting mPEG and MAC to give mPEG-*b*-PMAC copolymer followed by the addition of CB and LA [Scheme 1(A)]. A kinetic study was performed to determine the optimal time



SCHEME 1 Synthesis method for preparation of lactic acid- and carbonate-based crosslinked micelles. Conditions: (i) DBU, CH_2Cl_2 , RT, 3 h. (ii) AIBN, 60°C . (A) Interface-crosslinked micelles. (B) Core-crosslinked micelles.

required before the addition of CB and LA monomer. From Figure 2(A,B), a maximum MAC conversion of 80% was achieved at a time of 105 min and maintained at 120 min when DBU amount was $5 \mu\text{L}/\text{mL}$. The observed conversion saturation could possibly be due to lower MAC concentrations. A plot of $\ln(1/(1-x))$ versus time resulted in a straight line with a 70 min^{-1} rate constant. Since MAC conversion remained constant after 105 min, PEG-*b*-PMAC polymerization was carried for 2 h and characterized using ^1H NMR spectroscopy before the addition of CB and LA. A typical ^1H NMR spectrum for mPEG-*b*-PMAC copolymer is displayed in Figure 2(C).

The successful synthesis of mPEG-*b*-PMAC-*b*-P(CB-*co*-LA) copolymer was confirmed using ^1H NMR spectroscopy and GPC. The presence of characteristic resonance peaks for mPEG (3.65 ppm), LA (1.5–1.57, 5.12 ppm), CB (1.24, 4.25–4.35, 5.2, 7.3 ppm), and MAC (4.2–4.4, 4.6, 5.3–5.8 ppm) clearly confirmed the co-occurrence of all the monomers [Fig. 3(A)]. Some characteristics of the synthesized mPEG-*b*-PMAC-*b*-P(CB-*co*-LA) copolymer are summarized in Table 1. Copolymer molecular weight was determined by comparative analysis of the mPEG (i.e., $\text{CH}_2\text{-CH}_2\text{-}$ at 3.65 ppm), lactide (i.e., CH at 5.12), CB (i.e., C_6H_5 at 7.3 ppm), and MAC ($\text{-CH}_2\text{-CH=CH}_2$ at 5.8 ppm) characteristic proton peaks from ^1H NMR spectrum. mPEG-*b*-PMAC-*b*-P(CB-*co*-LA)

molecular weight was determined to be 10,558 g/mol from ^1H NMR spectrum. GPC measurements also confirmed successful copolymer synthesis and showed the resulting copolymer to have a PDI of 1.19 and M_n of 9462 g/mol.

Synthesis and Characterization of mPEG-*b*-P(CB-*co*-LA-*co*-MAC) Copolymer

The synthetic procedure for mPEG-*b*-P(CB-*co*-LA-*co*-MAC) copolymer is shown in Scheme 1(B). mPEG-*b*-P(CB-*co*-LA-*co*-MAC) copolymer was obtained by ring-opening polymerization (ROP) of CB, MAC, and LA using PEO as a macroinitiator and DBU as a catalyst. The monomer to initiator mole ratio was set at 20:1 with MAC monomer constituting 8 mol %. Addition of 5 mol % DBU resulted in greater than 80% monomer conversion in 3 h affording copolymer with controlled molecular weights and low polydispersity. ^1H NMR spectrum [Fig. 3(B)] of mPEG-*b*-P(CB-*co*-LA-*co*-MAC) copolymer showed the following resonance peaks at δ 3.65, 5.12, 5.28–5.8, and 7.3 attributable to the methylene protons of mPEG, the methylene protons of lactide, the acryloyl protons of MAC, and the phenyl protons of carbonate, respectively. Furthermore, the signals at 4.25–4.35 reflect the methylene protons in the carbonate main chain and confirm successful ROP of the carbonate monomers. The molecular weight of mPEG-*b*-P(CB-*co*-LA-*co*-MAC) copolymer was estimated to be 10,020 g/mol using the

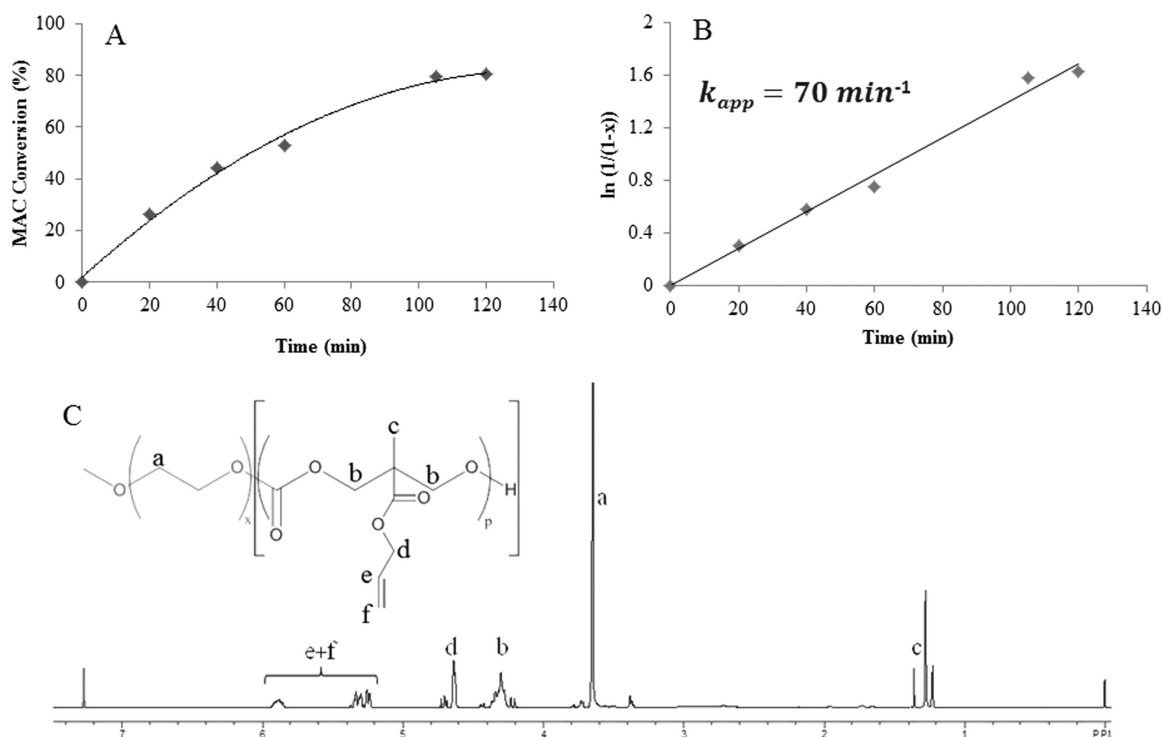


FIGURE 2 mPEG and MAC copolymerization in CH_2Cl_2 at room temperature. Reaction progress was monitored by ^1H NMR spectroscopy. (A) Observed MAC conversion during synthesis of mPEG-*b*-PMAC copolymer. (B) Plot of $\ln(1/(1-x))$ versus time (x = monomer conversion). (C) ^1H NMR spectrum of mPEG-*b*-PMAC copolymer in CDCl_3 .

mPEG ($\delta = 3.65$), LA ($\delta = 5.12$), CB ($\delta = 7.3$), and MAC ($\delta = 5.8$) characteristic peaks. GPC revealed mPEG-*b*-P(CB-*co*-LA-*co*-MAC) copolymer to have a polydispersity of 1.22

and M_n of 9875 g/mol which was close to the theoretical molecular weight and that determined by ^1H NMR spectroscopy.

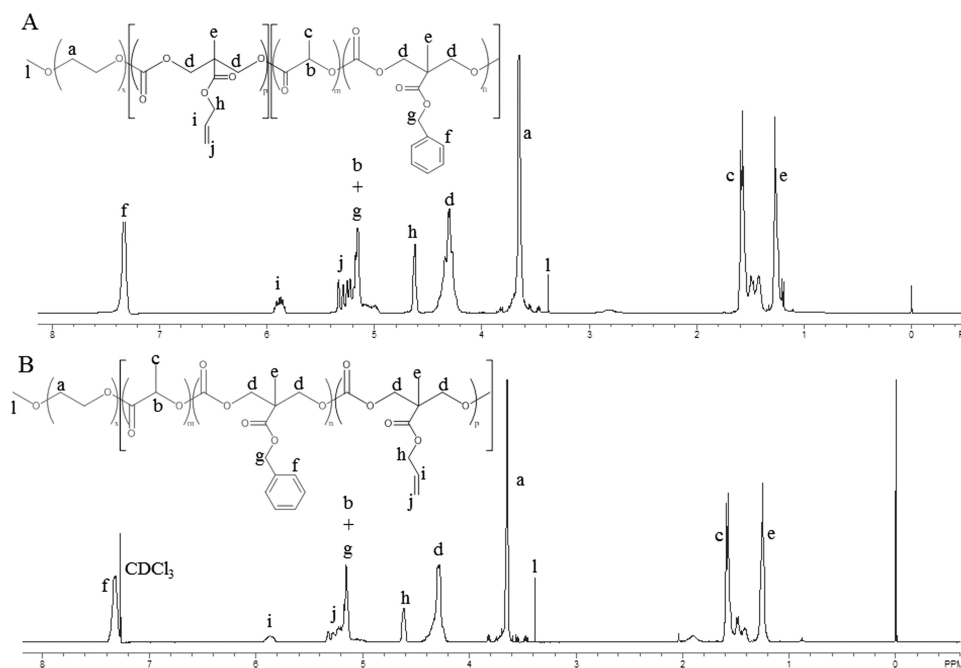


FIGURE 3 ^1H NMR spectra for lactic acid- and carbonate-based copolymer for crosslinked micelles. (A) mPEG-*b*-PMAC-*b*-P(CB-*co*-LA) copolymer in CDCl_3 . (B) mPEG-*b*-P(CB-*co*-LA-*co*-MAC) copolymer in CDCl_3 .

TABLE 1 Characteristics of Lactic Acid- and Carbonate-Based Copolymers

| Block Copolymer | M_n ($^1\text{H NMR}^a$) | M_n (GPC b) | M_w (GPC b) | M_w/M_n (GPC b) | CMC (g/l) |
|---|------------------------------|-------------------|-------------------|-----------------------|-----------|
| mPEG $_{114}$ - <i>b</i> -P(CB $_8$ - <i>co</i> -LA $_{35}$ - <i>co</i> -MAC $_{2.5}$) | 10,020 | 9,875 | 12,106 | 1.22 | 0.001 |
| mPEG $_{114}$ - <i>b</i> -PMAC $_{2.5}$ - <i>b</i> -P(CB $_9$ - <i>co</i> -LA $_{39}$) | 10,558 | 9,462 | 11,260 | 1.19 | 0.0008 |

^a Molecular weight calculated from $^1\text{H NMR}$ spectroscopy.^b Determined using GPC (polystyrene standards).**Microstructure Analysis and Polymer Toxicity**

MAC arrangement is expected to be blocky in mPEG-*b*-PMAC-*b*-P(CB-*co*-LA) and random in mPEG-*b*-P(CB-*co*-LA-*co*-MAC) copolymers. Since ^{13}C NMR spectroscopy is sensitive to chemical shifts of the quaternary carbon in the polymer backbone and secondary carbon in the side group, it was used to confirm MAC arrangement in both copolymers. The ^{13}C NMR spectra of mPEG-*b*-PMAC-*b*-P(CB-*co*-LA) and mPEG-*b*-P(CB-*co*-LA-*co*-MAC) copolymers are shown in Figure 4(A,B), respectively, and further confirm successful copolymer synthesis. However, to determine MAC monomer

arrangement, the ^{13}C NMR spectra of mPEG-*b*-PMAC, mPEG-*b*-PMAC-*b*-P(CB-*co*-LA), mPEG-*b*-P(CB-*co*-LA-*co*-MAC), and mPEG-*b*-P(CB-*co*-LA) copolymers were analyzed by observing peaks at 65.82 ppm (secondary carbon) and 46.48 ppm (quaternary carbon), respectively.

From Figure 5, a distinctive peak can be observed at 65.82 ppm for mPEG-*b*-PMAC copolymer synonymous with the secondary carbon on the allyl group. This characteristic peak at 65.82 ppm is also evident for mPEG-*b*-PMAC-*b*-P(CB-*co*-LA) copolymer suggesting the presence of mPEG-*b*-PMAC block in mPEG-*b*-PMAC-*b*-P(CB-*co*-LA) copolymer. The additional

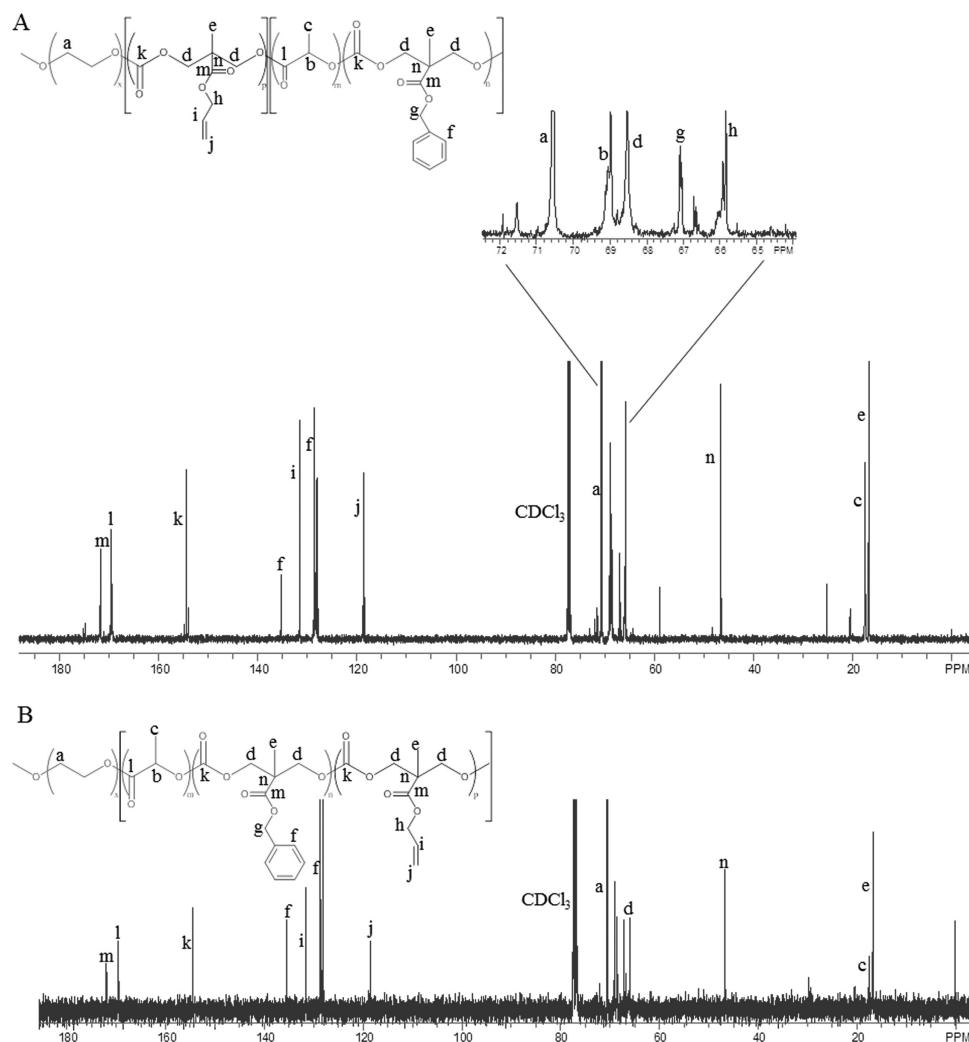


FIGURE 4 ^{13}C NMR spectra for lactic acid- and carbonate-based copolymer for crosslinked micelles. (A) mPEG-*b*-PMAC-*b*-P(CB-*co*-LA) copolymer in CDCl_3 . (B) mPEG-*b*-P(CB-*co*-LA-*co*-MAC) copolymer in CDCl_3 .

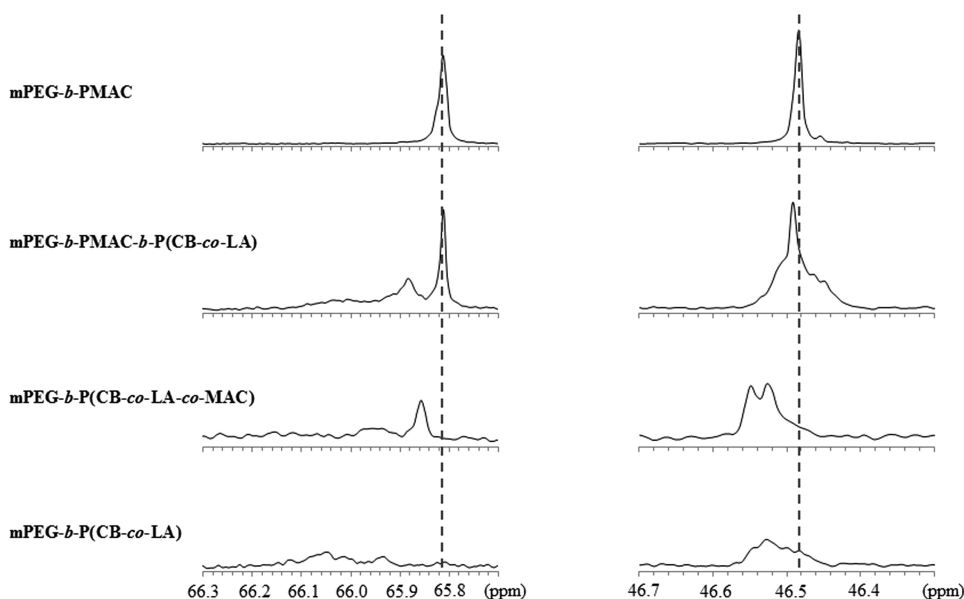


FIGURE 5 ^{13}C NMR spectra comparative plot for mPEG-*b*-PMAC, mPEG-*b*-PMAC-*b*-P(CB-*co*-LA), mPEG-*b*-P(CB-*co*-LA-*co*-MAC), and mPEG-*b*-P(CB-*co*-LA) demonstrating differences in monomer arrangement.

peak shifted downfield is assigned as the same carbon of MAC unit adjacent to P(CB-*co*-LA), which is reasonable since PMAC is short ($n = 2.5$). In contrast, the characteristic secondary carbon peak of MAC shifts downfield for mPEG-*b*-P(CB-*co*-LA-*co*-MAC) copolymer, indicating lack of MAC block sequence. This MAC peak is clearly absent in mPEG-*b*-P(CB-*co*-LA) copolymer. Furthermore, the 46.48 ppm peak representing the quaternary carbon in mPEG-*b*-PMAC main chain is seen in the spectra of mPEG-*b*-PMAC-*b*-P(CB-*co*-LA) copolymer. The same peak is seen for mPEG-*b*-PMAC-*b*-P(CB-*co*-LA) overlapped with the broad peak which is corresponding to the quaternary carbon from the CB unit. Unlike mPEG-*b*-PMAC and mPEG-*b*-PMAC-*b*-P(CB-*co*-LA), the 46.48 ppm peak is shifted downfield for mPEG-*b*-P(CB-*co*-LA-*co*-MAC) demonstrating random distribution of MAC monomer. A similar broad peak can be observed for mPEG-*b*-P(CB-*co*-LA) reflecting contribution from the CB quaternary carbon. As allyl compounds can be toxic, we evaluated the toxicity of mPEG-*b*-PMAC-*b*-P(CB-*co*-LA) and mPEG-*b*-P(CB-*co*-LA-*co*-MAC) copolymers in LNCaP prostate cancer cell lines. Our data reveal both copolymers are not toxic up to 2000 $\mu\text{g}/\text{mL}$ (Fig. 6). In this study, the effect of micelles (NCM and CM) on cancer cells was investigated to determine the influence of these delivery vehicles on cancer cell proliferation. This study confirmed that the therapeutic effect observed following treatment with drug-loaded micelles was as a result of the drug and not an artifact of the carrier.

Effect of Polymer Composition and MAC Location on CMC, Particle Size, and Drug Loading

Slight changes in polymer composition (e.g., monomer content and arrangement) can affect micelle properties. Therefore, we examined the effect of polymer composition, MAC location and crosslinking on CMC, size, and drug loading. The CMC of mPEG-*b*-P(CB-*co*-LA-*co*-MAC) was found to be

0.001 g/L. In contrast, mPEG-*b*-PMAC-*b*-P(CB-*co*-LA) had a CMC of 0.0008 g/L. These results when juxtaposed with our previous findings¹² suggests the presence of the intermediate MAC block results in copolymers that form more thermodynamically stable micelles compared to random distribution of MAC in the hydrophobic core.

Subsequently, micelle size and drug-loading content were determined following preparation by the film sonication method. We observed that the introduction of MAC monomer did not affect the micelle forming ability or morphology of the block copolymers regardless of its location. Micelle size and morphology were examined by DLS and TEM, respectively. Average hydrodynamic size was 123 ± 3.02 nm for

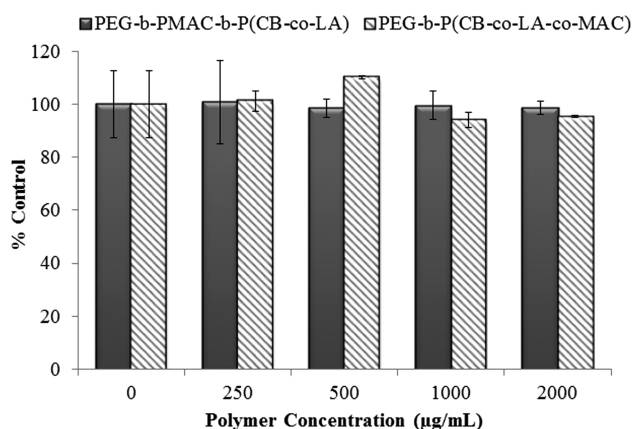


FIGURE 6 Cytotoxicity of mPEG-*b*-PMAC-*b*-P(CB-*co*-LA) and mPEG-*b*-P(CB-*co*-LA-*co*-MAC) copolymers in prostate cancer cells. LNCaP cells were incubated with various concentrations of copolymers (0–2000 $\mu\text{g}/\text{mL}$) for 48 h and cell viability was determined by MTT assay. Data are presented as mean \pm SD ($n = 3$).

TABLE 2 Effect of Polymer Composition and MAC Location on Particle Size and Drug Loading

| Block Copolymer ^a | Size (nm) ^c | PDI | Drug loading (%) ± SD ^b | Encapsulation Efficiency (%) ± SD |
|---|------------------------|-------------|------------------------------------|-----------------------------------|
| Non-crosslinked | | | | |
| Before drug loading | | | | |
| mPEG ₁₁₄ - <i>b</i> -P(CB ₈ - <i>co</i> -LA ₃₅ - <i>co</i> -MAC _{2.5}) | 123.0 ± 3.02 | 0.15 ± 0.01 | – | – |
| mPEG ₁₁₄ - <i>b</i> -PMAC _{2.5} - <i>b</i> -P(CB ₉ - <i>co</i> -LA ₃₉) | 128.0 ± 1.10 | 0.12 ± 0.01 | – | – |
| After drug loading | | | | |
| mPEG ₁₁₄ - <i>b</i> -P(CB ₈ - <i>co</i> -LA ₃₅ - <i>co</i> -MAC _{2.5}) | 139.0 ± 1.05 | 0.10 ± 0.02 | 3.79 ± 0.56 | 75.72 ± 0.15 |
| mPEG ₁₁₄ - <i>b</i> -PMAC _{2.5} - <i>b</i> -P(CB ₉ - <i>co</i> -LA ₃₉) | 133.0 ± 1.49 | 0.04 ± 0.01 | 1.01 ± 0.73 | 20.29 ± 0.11 |
| Crosslinked | | | | |
| Before drug loading | | | | |
| mPEG ₁₁₄ - <i>b</i> -P(CB ₈ - <i>co</i> -LA ₃₅ - <i>co</i> -MAC _{2.5}) | 151.0 ± 1.69 | 0.12 ± 0.04 | – | – |
| mPEG ₁₁₄ - <i>b</i> -PMAC _{2.5} - <i>b</i> -P(CB ₉ - <i>co</i> -LA ₃₉) | 135.0 ± 1.89 | 0.20 ± 0.03 | – | – |
| After drug loading | | | | |
| mPEG ₁₁₄ - <i>b</i> -P(CB ₈ - <i>co</i> -LA ₃₅ - <i>co</i> -MAC _{2.5}) | 118.0 ± 1.70 | 0.10 ± 0.01 | 3.21 ± 2.11 | 64.08 ± 0.48 |
| mPEG ₁₁₄ - <i>b</i> -PMAC _{2.5} - <i>b</i> -P(CB ₉ - <i>co</i> -LA ₃₉) | 122.0 ± 0.81 | 0.12 ± 0.01 | 0.89 ± 0.10 | 17.77 ± 0.02 |

^a Subscripts reflect degree of polymerization of each monomer obtained from ¹H NMR spectroscopy.

^b Percentage of drug loaded into micelles based on 5% theoretical loading.

^c Mean particle size was determined by dynamic light scattering.

mPEG-*b*-P(CB-*co*-LA-*co*-MAC) copolymer while that of mPEG-*b*-PMAC-*b*-P(CB-*co*-LA) was 128 ± 1.10 nm (Table 2) with both copolymers resulting in micelles possessing low PDI values (0.12–0.15; Table 2) implying a narrow micelle size distribution. Furthermore, our findings suggest inclusion of drug resulted in a modest increase in micelle size. Specifically, micelle size was 139 ± 1.05 nm for mPEG-*b*-P(CB-*co*-LA-*co*-MAC) copolymer while that of mPEG-*b*-PMAC-*b*-P(CB-*co*-LA) was 133 ± 1.49 nm. However, drug-loaded micelles still exhibited low PDI values.

We next quantified the amount of drug loaded into the micelles in terms of drug loading density (eq 1) and encapsulation efficiency (eq 2). From Table 2, mPEG-*b*-P(CB-*co*-LA-*co*-MAC) copolymer had superior drug loading characteristics compared to mPEG-*b*-PMAC-*b*-P(CB-*co*-LA). Based on a 5% theoretical loading, mPEG-*b*-P(CB-*co*-LA-*co*-MAC) had a drug loading density of 3.79% ± 0.56% indicating an encapsulation efficiency of 78.72% ± 0.15%. In contrast, drug loading density for mPEG-*b*-PMAC-*b*-P(CB-*co*-LA) was computed to be 1.01% ± 0.73% reflecting a 20.29% ± 0.11% encapsulation efficiency. Furthermore, surface charge of the micelles prepared from both copolymers were observed to be slightly negative: −0.96 ± 0.05 and −5.52 ± 0.13 mV for mPEG-*b*-P(CB-*co*-LA-*co*-MAC) and mPEG-*b*-PMAC-*b*-P(CB-*co*-LA), respectively.

Effect of Crosslinking on Particle Size, Morphology, and Drug Loading

Next, mPEG-*b*-P(CB-*co*-LA-*co*-MAC) and mPEG-*b*-PMAC-*b*-P(CB-*co*-LA) copolymers were suitably crosslinked in a mixture of THF and water at 70°C using AIBN as the initiator. Pendant allyl moieties in the core and interface of copolymers allowed convenient crosslinking in the presence of AIBN initiator. ¹H NMR and IR spectroscopy was used to confirm the success of crosslinking. As shown in Figure 7(A),

a prominent peak at δ5.8 ppm (acryloyl proton) can clearly be seen in the NCM. In contrast, the signal significantly weakened for the crosslinked sample (Fig. 7(B)). Quantitative analysis from the ¹H NMR spectra revealed 69% crosslinking efficiency. IR spectroscopy also confirmed successful crosslinking as indicated by the weakening of the 1650 cm^{−1} peak corresponding to the alkene group (Fig. 8).

From our studies, crosslinking of non-drug-loaded micelles generally led to an increase in micelle size compared to their non-crosslinked counterparts (Table 2). This size change was greater for mPEG-*b*-P(CB-*co*-LA-*co*-MAC) which increased from 123 ± 3.02 nm to 151 ± 1.69 nm compared to mPEG-*b*-PMAC-*b*-P(CB-*co*-LA) where size was 128 ± 1.10 nm and 135 ± 1.89 nm before and after crosslinking, respectively. Interestingly, we observed that crosslinking of drug-loaded micelles resulted in a decrease in size compared to their non-crosslinked counterparts (Table 2). Here again, the size change was greater for mPEG-*b*-P(CB-*co*-LA-*co*-MAC) compared to mPEG-*b*-PMAC-*b*-P(CB-*co*-LA) (21 nm vs. 11 nm). Our findings also suggest that crosslinking resulted in a modest decrease in drug loading regardless of copolymer type. Furthermore, TEM analysis demonstrates that crosslinking does not significantly alter micelle morphology (Fig. 9).

Effect of Crosslinking on Stability

After confirming successful crosslinking of micelles, we next examined the effect of crosslinking on micelle stability in physiologically relevant and extreme micelle destabilization conditions. Since micelles encounter sink-like conditions upon systemic administration, we first examined the stability of NCM and CM in PBS at micelle concentrations of 200, 20, 2, and 0.20 μg/mL. Both NCM and CM remained intact up to 2 μg/mL micelle concentration further demonstrating the thermodynamic stability of both micelle systems. Under these

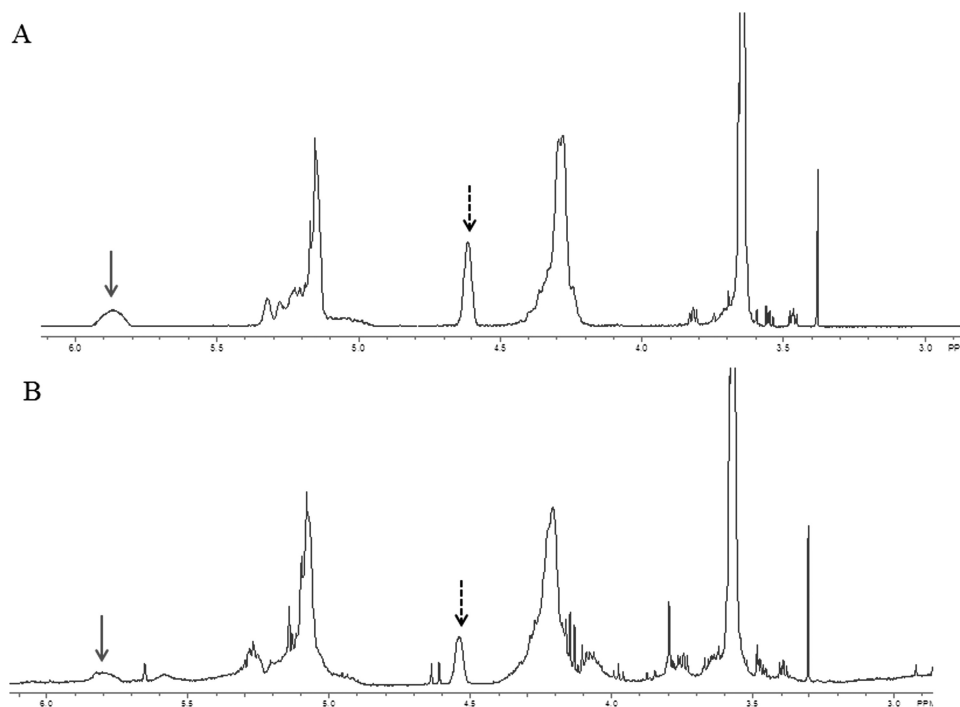


FIGURE 7 ^1H NMR spectra for mPEG-*b*-P(MAC-*co*-CB-*co*-LA) copolymer in CDCl_3 . (A) Before crosslinking. (B) After crosslinking.

conditions, NCM had an average size of 123 ± 3.02 nm with 0.15 ± 0.01 PDI while CM exhibited an average size of 127 ± 3.69 nm with 0.16 ± 0.02 PDI. However, the NCM dissociated when micelle concentration was $0.20 \mu\text{g}/\text{mL}$, whereas the CM maintained their nanostructure [Fig. 10(A)].

We next investigated the stability of micelles with or without drug in the presence of serum for 24 and 48 h. From Figure 10(B), NCM appeared to aggregate with time as indicated by increase in particle size. For example, the d_i/d_0 (diameter at specified time to diameter at $t = 0$) ratio increased from approximately 1 to 4 and 8 at 24 and 48 h, respectively. We also determined the CMC of mPEG-*b*-P(CB-*co*-LA-*co*-MAC) NCM and CM as a secondary measure of stability (Supporting Information). Our results reveal NCM had a CMC value of 1 mg/L based on where the two tangent lines intersect. In contrast, CMC of crosslinked micelles was determined to be 0.06 mg/L. These results demonstrate that CM enhanced stability compared to NCM.

In Vitro Release Studies of Bicalutamide from Polymeric Micelles

We next performed *in vitro* bicalutamide release study in PBS (pH 7.4) at 37°C and 150 rpm with 0.1% Tween-80 to determine the effect of crosslinking on drug release. Figure 11 shows the cumulative percentage of bicalutamide released from mPEG-*b*-P(CB-*co*-LA-*co*-MAC) and mPEG-*b*-PMAC-*b*-P(CB-*co*-LA) NCM and CM. Our results clearly reveal that the release of bicalutamide from mPEG-*b*-P(CB-*co*-LA-*co*-MAC) CM to be slower than their non-crosslinked counterpart. The cumulative amount of bicalutamide released after 72 h was $\sim 76\%$ for NCM and 60% for CM. However, $\sim 78\%$ of bicalutamide was released from NCM compared to 68% from CM in the case of mPEG-*b*-PMAC-*b*-P(CB-*co*-LA) copolymer.

In Vitro Cytotoxicity of mPEG-*b*-PMAC-*b*-P(CB-*co*-LA) and mPEG-*b*-P(CB-*co*-LA-*co*-MAC) NCM and CM

The inhibitory effect of bicalutamide-loaded mPEG-*b*-PMAC-*b*-P(CB-*co*-LA) and mPEG-*b*-P(CB-*co*-LA-*co*-MAC) NCM and CM was determined in LNCaP human prostate cancer cell line for 24 h. From Figure 12(A), bicalutamide-loaded

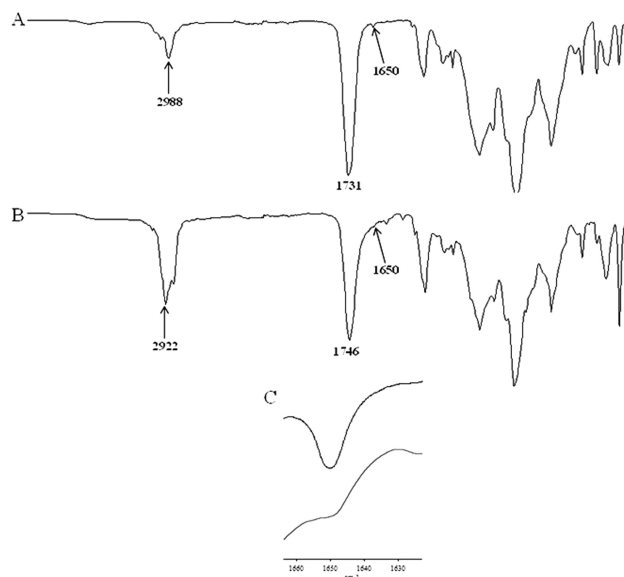


FIGURE 8 FTIR spectra for lactic acid- and carbonate-based copolymer (A) before crosslinking and (B) after crosslinking. Arrow indicates weakening of 1650 cm^{-1} peak reflecting crosslinking of double bonds. (C) Peaks at 1650 cm^{-1} zoomed in and offset for clarity; Top (before crosslinking) and Bottom (after crosslinking).

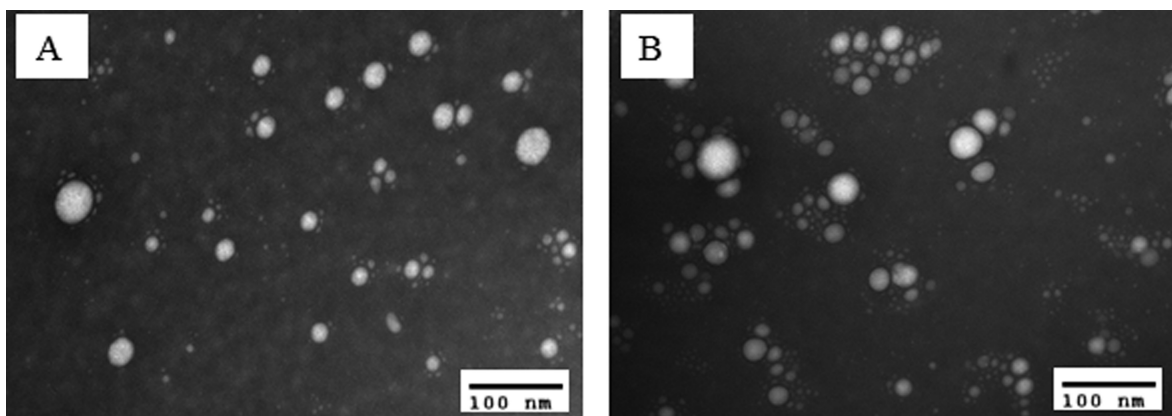


FIGURE 9 TEM images of (A) NCM and (B) CM.

crosslinked micelles more potently inhibited LNCaP cell growth compared to bicalutamide-loaded NCM regardless of polymer type. For bicalutamide-loaded mPEG-*b*-PMAC-*b*-P(CB-*co*-LA) micelles, IC₅₀ for NCM was ~47.2 μM while that of CM was ~15.0 μM. Similarly, bicalutamide-loaded mPEG-*b*-P(CB-*co*-LA-*co*-MAC) NCM had an IC₅₀ of ~36.9 μM while CM had IC₅₀ of ~15.4 μM. Bicalutamide is known to affect expression of prostate-specific antigen (PSA), which is downstream of and regulated by the androgen-androgen receptor signaling axis. Therefore, we examined the effect of bicalutamide-loaded CM and NCM on secreted PSA following incubation in LNCaP cells for 24 h. Our results suggests bicalutamide micelles reduce secreted PSA expression by approximately 50% compared to control, irrespective of polymer type and presence of crosslinking [Fig. 12(B)].

DISCUSSION

Polymeric micelles are promising drug delivery platforms.^{9,12,25,26,28–30} Insight accruing from micelle research particularly in oncology has led to the strategic design and synthesis of novel polymers to address the key issues of adequate drug loading, targetability, sustained drug release and degradation. Despite significant advances made in these

areas, one reason the pharmaceutical industry has not fully adopted micelle formulations is their perceived instability especially in biological environments. The purpose of our study is to address this pertinent issue through the synthesis, characterization, and *in vitro* evaluation of innovative lactic acid- and carbonate-based CM for enhanced drug delivery.

We have successfully synthesized mPEG₁₁₄-*b*-PMAC_{2.5}-*b*-P(CB₉-*co*-LA₃₉) and mPEG₁₁₄-*b*-P(CB₈-*co*-LA₃₅-*co*-MAC_{2.5}) copolymers for core-corona interface-crosslinked and core-crosslinked micelles, respectively (Scheme 1). The design of these copolymers was guided by our desire to improve upon the existing micelle properties obtained using our previously synthesized mPEG-*b*-P(CB-*co*-LA) copolymers, especially with regards to sub-CMC and serum stability. Therefore, we decided to strategically introduce chemical crosslinks at the core-corona interface with the goal of creating a molecular fence to improve micelle integrity and sustained release. We also introduced crosslinks in the core as a complimentary approach and to demonstrate the flexibility of our crosslinking approach. Although a variety of chemistries (e.g., click chemistry, disulfide bond) can be used for crosslinking, we judiciously selected the MAC monomer as our crosslinking

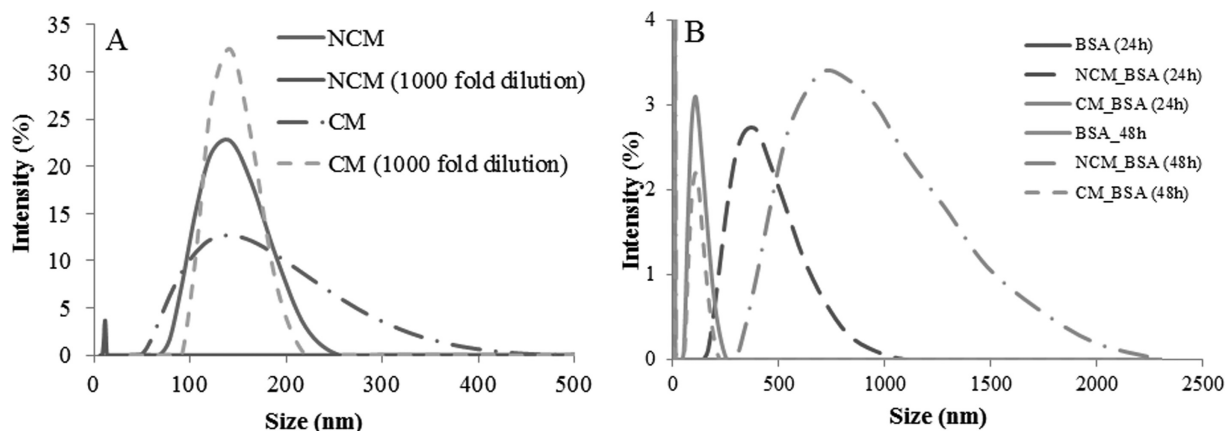


FIGURE 10 Stability of mPEG-*b*-PMAC-*b*-P(CB-*co*-LA) NCM and CM. (A) Micelle stability against 1000-fold dilution. (B) Micelle stability in BSA after 24 and 48 h.

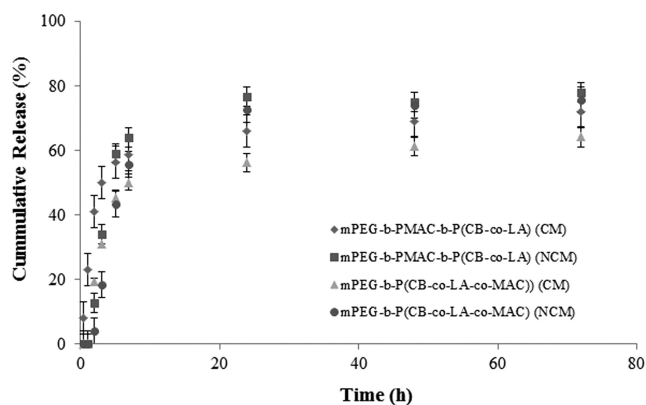


FIGURE 11 Effect of crosslinking on bicalutamide release from mPEG-*b*-PMAC-*b*-P(CB-*co*-LA) and mPEG-*b*-P(CB-*co*-LA-*co*-MAC) micelles. Release experiments were performed in triplicate in PBS with 0.1% Tween 80 at 37°C and 150 rpm.

moiety as we did not want to dramatically alter the superior attributes of mPEG-*b*-P(CB-*co*-LA) copolymer (e.g., drug loading, thermodynamic stability, micelle architecture, biodegradability). MAC has close structural similarity to our well-studied cyclic carbonate (CB) monomer except it has an allyl pendant group in contrast to the phenyl pendant of CB. Therefore, we were confident that the introduction of MAC will not significantly change the backbone or hydrophilic lipophilic balance of the polymer. We synthesized MAC monomer using two approaches (Fig. 1) and used ¹H NMR and FTIR spectrometry to confirm its structure. No FTIR data was found in the literature, however, our ¹H NMR spectrum matched the literature.²⁰ While the first approach had a shorter overall reaction time, the second approach was preferred as it resulted in higher MAC yields (70% vs. 30%) and had fewer steps (2 vs. 4). Our MAC yield of 70% was comparable to that reported by Hu et al.²⁰ Furthermore, unlike the first approach which required column chromatography, pure compounds could be obtained with recrystallization in the second approach making it less labor intensive. Recently, Chen et al.³¹ also synthesized a couple of cyclic carbonate monomers similar to MAC. However, their synthetic scheme required four steps with overall yields of 40% which is lower than our preferred second approach.

mPEG-*b*-P(CB-*co*-LA) copolymers previously synthesized using Sn(Oct)₂ catalyzed ROP exhibited relatively high PDIs (around 1.4) possibly due to undesired transesterification.¹² Furthermore, increasing CB content affected LA reactivity. Therefore, we used the organic base catalyst DBU (pK_a = 24.3)³² for synthesizing mPEG₁₁₄-*b*-PMAC_{2.5}-*b*-P(CB₉-*co*-LA₃₉) and mPEG₁₁₄-*b*-P(CB₈-*co*-LA₃₅-*co*-MAC_{2.5}) copolymers. DBU is known to mitigate unwanted transesterification resulting in polymers with well-controlled molecular weights and low PDIs. In synthesizing mPEG₁₁₄-*b*-PMAC_{2.5}-*b*-P(CB₉-*co*-LA₃₉), we first sought to understand how the reactivity of MAC compares with CB using mPEG as a macroinitiator. Our findings suggest the reactivity of MAC (80% conversion in 2 h (Fig. 2)) to be similar to that of CB (data not shown) indicating the pendant group does not significantly impact the

reactivity of the cyclic carbonate monomers. The DBU-catalyzed conversion of our cyclic carbonates is higher than that of trimethyl carbonate (80% vs. 70%) reported by Watanabe et al.;³³ however, they used 4-(chloromethyl)benzyl alcohol as an initiator. Our kinetic study suggests MAC polymerization to be first order as demonstrated by the linear nature of the ln(1/(1 - x)) versus time plot [Fig. 2(B)]. This result is not surprising as DBU and mPEG concentrations do not change during polymerization. Qian et al.³⁴ have reported similar first-order dependency with respect to monomer, DBU, and macroinitiator concentrations for ROP of LA and glycolide.³⁴ Furthermore, ROP of valerolactone using similar amidine catalysts have been shown to follow first-order kinetics with respect to catalyst, alcohol, initiator and monomer concentration.³⁵ Although we did not systematically study the polymerization kinetics upon addition of CB and LA, a time of 3 h was sufficient to obtain polymers with targeted mass ratios of MAC, CB, and LA for both mPEG₁₁₄-*b*-PMAC_{2.5}-*b*-P(CB₉-*co*-LA₃₉) and mPEG₁₁₄-*b*-P(CB₈-*co*-LA₃₅-*co*-MAC_{2.5}) copolymers (inferred from ¹H NMR spectra).

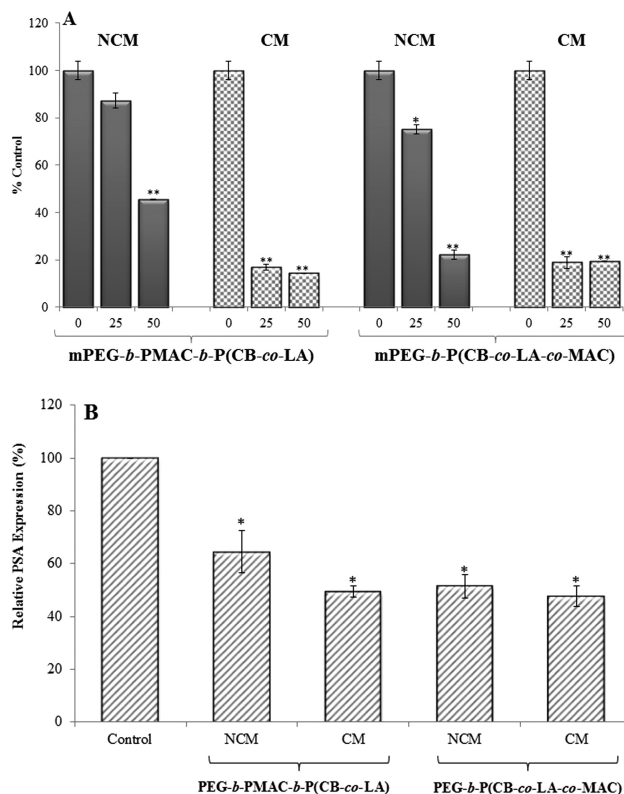


FIGURE 12 Anticancer effect of mPEG-*b*-PMAC-*b*-P(CB-*co*-LA) and mPEG-*b*-P(CB-*co*-LA-*co*-MAC) NCM and CM. (A) 3 × 10³ LNCaP cells were incubated with bicalutamide-loaded micelle formulations (0, 25, and 50 μM of drug) for 24 h. Cell viability was determined using MTT assay and results represented as the mean ± SD of triplicates. **p* < 0.05; ***p* < 0.01 using Student's unpaired *t* test. (B) Effect of bicalutamide-loaded mPEG-*b*-PMAC-*b*-P(CB-*co*-LA) and mPEG-*b*-P(CB-*co*-LA-*co*-MAC) NCM and CM (50 μM of drug) on secreted PSA following 24 h incubation.

Furthermore, DBU-catalyzed polymerization allowed us to obtain polymers in a relatively short time and avoided MAC crosslinking observed during initial polymerization studies attempted using Sn(Oct)₂ at 120°C.

Monomer arrangement in a copolymer significantly impacts its physicochemical properties and consequently key micelle properties. Consequently, we performed microstructure analysis on mPEG₁₁₄-*b*-PMAC_{2.5}-*b*-P(CB₉-*co*-LA₃₉) and mPEG₁₁₄-*b*-P(CB₈-*co*-LA₃₅-*co*-MAC_{2.5}) copolymers to confirm MAC arrangement in the copolymers. By systematically observing the shift in 65.82 ppm (secondary carbon) and 46.48 ppm (quaternary carbon) peaks in the ¹³C NMR spectra of mPEG-*b*-PMAC, mPEG-*b*-PMAC-*b*-P(CB-*co*-LA), mPEG-*b*-P(CB-*co*-LA-*co*-MAC), and mPEG-*b*-P(CB-*co*-LA) copolymers, we were able to show MAC arrangement to be block in mPEG-*b*-PMAC-*b*-P(CB-*co*-LA) and random in mPEG-*b*-P(CB-*co*-LA-*co*-MAC). Typically, reported microstructure analyses of ester-based copolymers use the carbonyl group in the polymer main chain. However, the close similarity between the contribution of MAC and CB to copolymer backbone complicates such analysis, and it is not feasible to use carbonyl groups in the polymer backbone for microstructure analysis in this study.

Although inclusion of MAC monomer added a layer of complexity in terms of microstructure analysis, our results suggest that it does not detrimentally affect micelle forming ability or key properties. Both mPEG₁₁₄-*b*-PMAC_{2.5}-*b*-P(CB₉-*co*-LA₃₉) and mPEG₁₁₄-*b*-P(CB₈-*co*-LA₃₅-*co*-MAC_{2.5}) micelles exhibited similar size (with or without drug), which was slightly larger than mPEG-*b*-P(CB-*co*-LA) micelles prepared in our previous study.¹² As micelle size is dependent on core composition and length (molecular weight), it appears this increase may be due to the contribution of the MAC monomer and relatively larger quantities of LA present in mPEG₁₁₄-*b*-PMAC_{2.5}-*b*-P(CB₉-*co*-LA₃₉) and mPEG₁₁₄-*b*-P(CB₈-*co*-LA₃₅-*co*-MAC_{2.5}) copolymers compared to mPEG₁₁₄-*b*-P(CB₈-*co*-LA₂₄) and mPEG₁₁₄-*b*-P(CB₉-*co*-LA₅) copolymers. Our results are consistent with the fact that hydrophobic blocks with higher molecular weight have generally been shown to have larger sizes. Notwithstanding, drug loading and encapsulation efficiency in crosslinked micelles were comparable to mPEG₁₁₄-*b*-P(CB₈-*co*-LA₂₄) and mPEG₁₁₄-*b*-P(CB₉-*co*-LA₅) micelles possessing similar CB content. The difference in bicalutamide loading between mPEG₁₁₄-*b*-PMAC_{2.5}-*b*-P(CB₉-*co*-LA₃₉) and mPEG₁₁₄-*b*-P(CB₈-*co*-LA₃₅-*co*-MAC_{2.5}) micelles may be attributed to CB content. Our previous studies clearly showed that CB degree of polymerization (DP) of nine resulted in a precipitous decrease in bicalutamide loading compared to DP of 8.¹² Furthermore, our results provide indirect evidence supporting our hypothesis that the structure and quantities of MAC present in the copolymer do not significantly alter drug loading characteristics.

Interestingly, mPEG₁₁₄-*b*-PMAC_{2.5}-*b*-P(CB₉-*co*-LA₃₉) and mPEG₁₁₄-*b*-P(CB₈-*co*-LA₃₅-*co*-MAC_{2.5}) micelles exhibited CMCs better than or comparable to mPEG-*b*-P(CB-*co*-LA) micelles with similar CB content suggesting equivalent if not better thermodynamic stability. Specifically, mPEG₁₁₄-*b*-

PMAC_{2.5}-*b*-P(CB₉-*co*-LA₃₉) micelles had a CMC of 0.0008 g/L while previously reported CMC of mPEG₁₁₄-*b*-P(CB₉-*co*-LA₅) micelles was 0.004 g/L. As CB content is the same in both copolymers, this fivefold improvement in CMC value is due to the presence of MAC and LA. However, CMC depends on both composition and molecular mass of the hydrophobic core.^{36,37} Therefore, it is difficult to clearly ascertain the individual contribution of MAC due to considerable difference in overall core length between mPEG₁₁₄-*b*-PMAC_{2.5}-*b*-P(CB₉-*co*-LA₃₉) (*M*_n = 9992 g/mol) and mPEG₁₁₄-*b*-P(CB₉-*co*-LA₅) (*M*_n = 7510 g/mol). Additionally, mPEG₁₁₄-*b*-P(CB₈-*co*-LA₃₅-*co*-MAC_{2.5}) micelles had a CMC of 0.001 g/L compared to 0.002 g/L for mPEG₁₁₄-*b*-P(CB₈-*co*-LA₂₄) micelles reported previously. Here, the modest improvement is most likely due to the presence of MAC since CB content is the same and the LA amounts are relatively close. Our results demonstrate that the CMC of mPEG₁₁₄-*b*-PMAC_{2.5}-*b*-P(CB₉-*co*-LA₃₉) and mPEG₁₁₄-*b*-P(CB₈-*co*-LA₃₅-*co*-MAC_{2.5}) micelles is sensitive to the presence of MAC but more importantly to its location and arrangement: block versus random distribution among CB and LA.

Crosslinking based on double bonds requires a radical initiator and exposure to heat or UV light. Our copolymers were successfully crosslinked using AIBN as radical initiator at a temperature of 70°C for 24 h. We observed crosslinking efficiency of approximately 70% which was slightly lower than the 80% value reported in the literature.²³ Complete crosslinking may not be possible as all the allyl moieties present will have to be in close proximity for this to occur. However, it is unlikely that micelle architecture would permit all the double bonds to be within the effective distance required for crosslinking. Theoretically, a few rightly positioned crosslinks would be sufficient to improve micelle mechanical integrity and 10 % crosslinking efficiency is not required. We found that crosslinking of blank micelles caused a modest increase in size. This we believe may be an artifact of the crosslinking process as THF used in the process is known to cause micelles to swell. Unexpectedly, crosslinking of drug-loaded micelles resulted in a decrease in micelle size regardless of MAC location. This was accompanied by a small loss in drug loading and encapsulation efficiency post-crosslinking. The reduction in drug loading and encapsulation efficiency may be due to leakage during the crosslinking process and may account for the modest size decrease observed after crosslinking. Finally, it is worth mentioning that while the CM possess better mechanical integrity than the non-crosslinked counterparts they are designed ultimately to be biodegradable. The polymer main chain consists of ester linkage and carbonate linkage, which degrades enzymatically regardless of side-chain crosslinking. The number of crosslinkable monomers in these polymers is limited to 2–3 units, thus we do not expect any long polymerization to occur by crosslinking reaction in the micelle form. However, further studies investigating the actual structure of the crosslinked micelles, biodegradability, and their safety are required.

Polymeric micelles are dynamic in nature and gradually disintegrate under sub-CMC conditions. Therefore, monitoring

changes in micelle size (using DLS) at different dilutions is an elegant way to determine micelle stability. Our results reveal that CM remain intact even below the CMC [Fig. 8(A)] while NCM disintegrated. CMC for CM was found to be 20-fold lower compared to NCM confirming the fact that CM were several times more stable than their non-crosslinked counterparts. It is worth mentioning that, although CMC of CM has little practical meaning it still provides a reasonable measure of the extent in improvement in micelle mechanical integrity. Micelles have also been shown to become unstable once they encounter blood components.^{11,36,38} Instability may result from protein adsorption, protein penetration, or drug extraction.³⁶ As the most abundant protein in blood plasma is serum albumin, we investigated the effect of physiological simulating concentrations of BSA (45 mg/mL) on CM and NCM stability using DLS to observe time-dependent changes in micelle size. Our results showed significant increase in size of NCM with time and reflect aggregation of micelles in BSA. This phenomenon may be due to protein adsorption which is undesirable as it can result in fast clearance by the mononuclear phagocyte system.³⁹ It has been shown that BSA–micelle interaction is typically driven by hydrophobic aggregation. For instance, micelles with high density hydrophilic corona experience greater steric stabilization and encounter less BSA interaction.⁴⁰ Other instances of polymeric micelle aggregation and interaction with BSA have been reported in the literature.^{40,41} In contrast, there was no appreciable increase in the size of CM following incubation with BSA. One reason may be the less dynamic nature of CM, which limits the continuous interchange of unimers thereby reducing the possibility of BSA interacting with the hydrophobic core. It is also likely that the presence of covalent crosslinks make it difficult for BSA to disrupt micelle architecture thus preventing BSA–micelle aggregates.

CONCLUSIONS

To address the current need for biodegradable, biocompatible, and stable polymeric micelle delivery systems, we report on the synthesis, characterization, and evaluation of lactic acid- and carbonate-based copolymers containing an allyl moiety for preparing interface and core crosslinked micelles. A series of complimentary spectroscopic techniques was used to confirm successful synthesis by ROP, elucidate polymer microstructure, and confirm crosslinking. mPEG₁₁₄-b-PMAC_{2.5}-b-P(CB₉-co-LA₃₉) and mPEG₁₁₄-b-P(CB₈-co-LA₃₅-co-MAC_{2.5}) copolymers for interface and core crosslinking, respectively, exhibited relatively low PDI (1.19–1.22) and CMC values (0.8–1 mg/L). Inclusion of MAC monomer did not significantly alter micelle size or morphology irrespective of polymer composition or MAC location. Importantly, mPEG₁₁₄-b-P(CB₈-co-LA₃₅-co-MAC_{2.5}) had a higher drug encapsulation efficiency (78.72% ± 0.15%) compared to mPEG₁₁₄-b-PMAC_{2.5}-b-P(CB₉-co-LA₃₉) (20.29% ± 0.11%). Subsequent micelle crosslinking did not dramatically change drug loading or micelle morphology. However, there was a strong link between micelle crosslinking and improved stability when incubated in aqueous media under extensive

dilution and physiological simulating serum (BSA ~45 mg/mL). CM size remained unchanged while NCM disintegrated at a thousand fold dilution. Besides, CM size remained unchanged in BSA whereas there was a time-dependent increase in the size of NCM. These results showed CM to be more stable compared to their non-crosslinked counterparts. Additionally, bicalutamide-loaded CM were found to be more potent in inhibiting proliferation of LNCaP prostate cancer cells compared to NCM regardless of polymer type. In all, we have demonstrated that these new biodegradable copolymer systems are potentially useful for cancer therapy. Future studies on influence of MAC block length, extent of crosslinking efficiency, and ratio of MAC to CB and LA on key micelle properties are required to generate material design rules which can be used for customized fabrication of improved micelle delivery platforms.

ACKNOWLEDGMENT

This work is supported by an Idea Award (W81XWH-10-1-0969) from the Department of Defense Prostate Cancer Research Program.

REFERENCES AND NOTES

- 1 Kwon, G. S. *Crit. Rev. Ther. Drug Carrier Syst.* **2003**, *20*, 357–403.
- 2 Soga, O.; van Nostrum, C. F.; Fens, M.; Rijcken, C. J.; Schiffelers, R. M.; Storm, G.; Hennink, W. E. *J Control Release* **2005**, *103*, 341–353.
- 3 Torchilin, V. P. *Pharm. Res.* **2007**, *24*, 1–16.
- 4 Solink, S.; Illum, L.; Davus, S. S. *Adv. Drug Deliv. Rev.* **1995**, *16*, 195–214.
- 5 Iyer, A. K.; Khaled, G.; Fang, J.; Maeda, H. *Drug Discov. Today* **2006**, *11*, 812–818.
- 6 Maeda, H. *Adv. Enzyme Regul.* **2001**, *41*, 189–207.
- 7 Matsumura, Y.; Maeda, H. *Cancer Res.* **1986**, *46* (12 Pt 1), 6387–6392.
- 8 Bronich, T. K.; Keifer, P. A.; Shlyakhtenko, L. S.; Kabanov, A. V. *J. Am. Chem. Soc.* **2005**, *127*, 8236–8237.
- 9 Lavanifar, A.; Samuel, J.; Kwon, G. S. *Adv. Drug Deliv. Rev.* **2002**, *54*, 169–190.
- 10 Liu, J.; Zeng, F.; Allen, C. J. *Control Release* **2005**, *103*, 481–497.
- 11 Savic, R.; Azzam, T.; Eisenberg, A.; Maysinger, D. *Langmuir* **2006**, *22*, 3570–3578.
- 12 Danquah, M.; Fujiwara, T.; Mahato, R. I. *Biomaterials* **2010**, *31*, 2358–2370.
- 13 Rosler, A.; Vandermeulen, G. W.; Klok, H. A. *Adv. Drug Deliv. Rev.* **2001**, *53*, 95–108.
- 14 Joralemon, M. J.; Murthy, K. S.; Remsen, E. E.; Becker, M. L.; Wooley, K. L. *Biomacromolecules* **2004**, *5*, 903–913.
- 15 O'Reilly, R. K.; Hawker, C. J.; Wooley, K. L. *Chem. Soc. Rev.* **2006**, *35*, 1068–1083.
- 16 Read, E. S.; Armes, S. P. *Chem. Commun. (Camb)* **2007**, 3021–3035.
- 17 Hawker, C. J.; Wooley, K. L. *Science* **2005**, *309*, 1200–1205.
- 18 Iijima, M.; Nagasaki, Y.; Okada, T.; Kato, M.; Kataoka, K. *Macromolecules* **1999**, *32*, 1140–1146.

- 19** Kim, J.-H.; Emoto, K.; Iijima, M.; Nagasaki, Y.; Aoyagi, T.; Okano, T.; Sakurai, Y.; Kataoka, K. *Polym. Adv. Technol.* **1999**, *10*, 647–654.
- 20** Hu, X.; Chen, X.; Xie, Z.; Liu, S.; Jing, X. *J. Polym. Sci.: Part A: Polym. Chem.* **2007**, *45*, 5518–5528.
- 21** Garg, S. M.; Xiong, X.-B.; Lu, C.; Lavasanifar, A. *Macromolecules* **2011**, *44*, 2058–2066.
- 22** Butun, V.; Wang, X.-S.; de Paz Banez, M. V.; Robinson, K. L.; Billingham, N. C.; Armes, S. P.; Tuzar, Z. *Macromolecules* **1999**, *33*, 1–3.
- 23** Hu, X.; Chen, X.; Wei, J.; Liu, S.; Jing, X. *Macromol. Biosci.* **2009**, *9*, 456–463.
- 24** Yang, R.; Meng, F.; Ma, S.; Huang, F.; Liu, H.; Zhong, Z. *Bio-macromolecules* **2011**, *12*, 3047–55.
- 25** Li, F.; Danquah, M.; Mahato, R. I. *Biomacromolecules* **2010**, *11*, 2610–2620.
- 26** Danquah, M.; Li, F.; Duke, C. B., 3rd; Miller, D. D.; Mahato, R. I. *Pharm. Res.* **2009**, *26*, 2081–2092.
- 27** Pratt, R. C.; Nederberg, F.; Waymouth, R. M.; Hedrick, J. L. *Chem. Commun. (Camb)* **2008**, 114–116.
- 28** Danquah, M.; Duke, C. B., 3rd; Patil, R.; Miller, D. D.; Mahato, R. I., Combination Therapy of Antiandrogen and XIAP Inhibitor for Treating Advanced Prostate Cancer. *Pharm. Res.* **2012**, *29*, 2079–2091.
- 29** Danquah, M. K.; Zhang, X. A.; Mahato, R. I. *Adv. Drug Deliv. Rev.* **2011**, *63*, 623–639.
- 30** Li, F.; Danquah, M.; Singh, S.; Wu, H.; Mahato, R. I. *Drug Deliv. Transl. Res.* **2011**, *1*, 420–428.
- 31** Chen, W.; Yang, H.; Wang, R.; Cheng, R.; Meng, F.; Wei, W.; Zhong, Z. *Macromolecules* **2010**, *43*, 201–207.
- 32** Kaljurand, I.; Kutt, A.; Soovali, L.; Rodima, T.; Maemets, V.; Leito, I.; Koppel, I. A. *J. Org. Chem.* **2005**, *70*, 1019–1028.
- 33** Watanabe, J.; Amemori, S.; Akashi, M. *Polymer* **2008**, *49*, 3709–3715.
- 34** Qian, H.; Wohl, A. R.; Crow, J. T.; Macosko, C. W.; Hoye, T. R. *Macromolecules* **2011**, *44*, 7132–7140.
- 35** Lohmeijer, B. G. G.; Pratt, R. C.; Leibfarth, F.; Logan, J. W.; Long, D. A.; Dove, A. P.; Nederberg, F.; Choi, J.; Wade, C.; Waymouth, R. M.; Hedrick, J. L. *Macromolecules* **2006**, *39*, 8574–8583.
- 36** Kim, S.; Shi, Y.; Kim, J. Y.; Park, K.; Cheng, J. X. *Expert Opin. Drug Deliv.* **2010**, *7*, 49–62.
- 37** Attwood, D.; Booth, C.; Yeates, S. G.; Chaibundit, C.; Ricardo, N. M. *Int. J. Pharm.* **2007**, *345*, 35–41.
- 38** Chen, H.; Kim, S.; He, W.; Wang, H.; Low, P. S.; Park, K.; Cheng, J. X. *Langmuir* **2008**, *24*, 5213–7.
- 39** Alexis, F.; Pridgen, E.; Molnar, L. K.; Farokhzad, O. C. *Mol. Pharm.* **2008**, *5*, 505–515.
- 40** Li, W.; Nakayama, M.; Akimoto, J.; Okano, T. *Polymer* **2011**, *52*, 3783–3790.
- 41** Yang, C.; Attia, A. B.; Tan, J. P.; Ke, X.; Gao, S.; Hedrick, J. L.; Yang, Y. Y. *Biomaterials* **2012**, *33*, 2971–2979.